Steel and Composite Structures, *Vol. 19, No. 6 (2015) 1403-1419*
DOI: http://dx.doi.org/10.12989/scs.2015.19.6.1403

Racking shear resistance of steel frames with corner connected precast concrete infill panels

J.C.D. Hoenderkamp*, H.H. Snijder [a] and H. Hofmeyer [b]

Department of the Built Environment, Eindhoven University of Technology, 5600MB Eindhoven, The Netherlands

(*Received May 27, 2013, Revised February 25, 2015, Accepted June 11, 2015*)

Abstract. When precast concrete infill panels are connected to steel frames at discrete locations, interaction at the structural interface is neither complete nor absent. The contribution of precast concrete infill panels to the lateral stiffness and strength of steel frames can be significant depending on the quality, quantity and location of the discrete interface connections. This paper presents preliminary experimental and finite element results of an investigation into the composite behaviour of a square steel frame with a precast concrete infill panel subject to lateral loading. The panel is connected at the corners to the ends of the top and bottom beams. The Frame-to-Panel-Connection, FPC4 between steel beam and concrete panel consists of two parts. A T-section with five achor bars welded to the top of the flange is cast in at the panel corner at a forty five degree angle. The triangularly shaped web of the T-section is reinforced against local buckling with a stiffener plate. The second part consists of a triangular gusset plate which is welded to the beam flange. Two bolts acting in shear connect the gusset plate to the web of the T-section. This way the connection can act in tension or compression. Experimental pull-out tests on individual connections allowed their load deflection characteristics to be established. A full scale experiment was performed on a one-storey one-bay 3 by 3 m infilled frame structure which was horizontally loaded at the top. With the characteristics of the frame-to-panel connections obtained from the experiments on individual connections, finite element analyses were performed on the infilled frame structures taking geometric and material non-linear behaviour of the structural components into account. The finite element model yields reasonably accurate results. This allows the model to be used for further parametric studies.

Keywords: racking shear resistance; infilled steel frame; concrete panel; panel-to-frame connection; full scale tests; finite element model

1. Introduction

The employment of discretely connected precast concrete panels in simple steel frames is very beneficial and results in a substantial increase in lateral stiffness and strength. When subjected to an in-plane horizontal load, the infill in steel framed structures will introduce different types of composite behaviour depending on the way it is attached to the steel frame as shown in Fig. 1.

*Corresponding author, Associate Professor Emeritus, E-mail: jcdh65@gmail.com
[a] Full Professor, E-mail: h.h.snijder@tue.nl
[b] Associate Professor, E-mail: h.hofmeyer@tue.nl

http://www.techno-press.org/?journal=scs&subpage=8 ISSN: 1229-9367 (Print), 1598-6233 (Online)

Since the early fifties research has been carried out on the structural behaviour of steel frames with masonry infill (Thomas 1953, Benjamin and Williams 1958, Polyakov 1960, Holmes 1961) and concrete(like) infill (Holmes 1961, Stafford Smith 1962, 1966). The infill used to be considered as a non-structural element, thereby neglecting its significant structural benefits. It was also shown (Stafford Smith 1967) that ignoring the infill may cause certain elements in the lower parts of the structure to be overloaded. If connections such as strong bonding or shear connectors at the structural interface between the frame and infill are absent as for example with brick infill, the structure can be classified as a non-integral infilled frame, see Fig. 1(a). Experimental investigations on non-integral infilled frames under racking load have shown (Stafford Smith 1962, 1966, 1967, Barua and Mallick 1977, Liauw and Kwan 1984, Liauw and Lo 1988, Ng'andu *et al*. 2006) that poor interaction between the frame and infill due to the absence of connectors or bonding causes friction at the structural interface. As the infill panel takes a large portion of the lateral load at its loaded corners, the effects of the infill panel are similar to the action of a single diagonal strut in compression bracing the frame. This analogy is justified by the phenomenon of slip and separation at the interface between the frame and the infill due to the difference in the deformed shapes of the surrounding steel frame and the brick infill. As a result, friction-slip at the interface becomes a governing factor in a non-integral infilled frame. The separation in addition to irregularities and unevenness at the structural interface produce considerable variations in strength and stiffness (Dawe and Seah 1989).

When a continuous connection is provided by means of strong bonding or shear connectors at the structural interface between frame and infill panel as shown in Fig. 1(b), the separation at the interface will be restricted and the performance of infilled frames is improved. Such frames are classified as fully-integral infilled frames. Friction-slip, which is dependent on normal stress, will not play an important role in fully-integral infilled frames. In addition, the provision of shear connectors overcomes the problem of an initial gap (lack of fit) at the interface. In general, fully-integral infilled frames have larger lateral stiffness and strength than non-integral infilled frames (Mallick and Garg 1971). They maintain their strength up to large deflections before final collapse of the structure.

When a precast concrete infill panel is connected to a steel frame at discrete locations as shown in Fig. 1(c), interaction at the structural interface is neither complete nor absent. A structure comprising a steel frame with an intermittently connected precast concrete panel can be classified as semi-integral. The contribution of precast concrete infill panels to the lateral stiffness and strength of steel frames depends on the quality, quantity and location of the discrete interface connections. The idea of a semi-integral infilled steel frame was considered earlier (Liauw and Kwan 1983) for an infilled frame with continuous connections along the beams and columns,

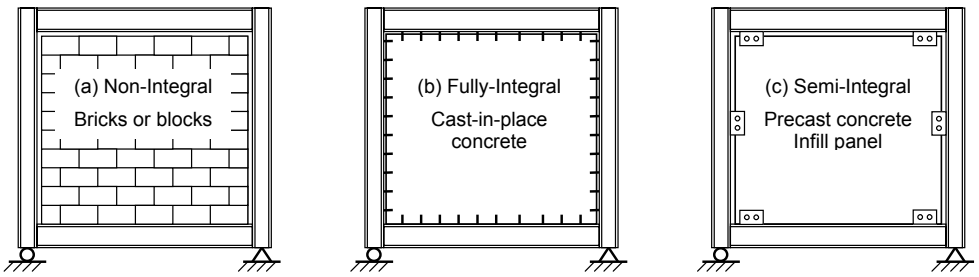

Fig. 1 Types of infilled steel frames

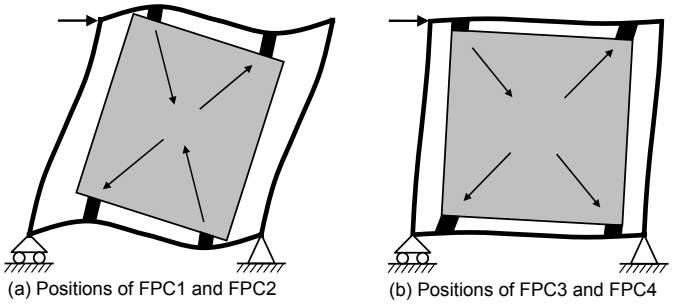

Fig. 2 Precast concrete infill panels in steel frames

where a finite shear strength at the steel-concrete interface was taken into account over specified lengths. Fig. 2(a) shows a deformed infilled frame with a panel connected to the beams of the steel frame. The use of discrete frame-to-panel connections means that contact only occurs at the frame-panel connections where the forces from the steel frame are introduced into the concrete. This way the infill panel functions as a bracing system with compression and tension forces (Hoenderkamp *et al*. 2010).

As part of this research program, two types of semi-integral infilled steel frames with discretely connected precast concrete infill panels were developed, tested and numerically investigated earlier: type one frames have connections that are able to transfer tension, shear as well as compression (Hoenderkamp *et al*. 2010), and type two frames with connections that can only transfer compressive forces (Teeuwen *et al*. 2008, 2010). For the study of type one infilled frames, two different frame-panel-connections were used: FPC1 and FPC2 connected to the beams as shown in Fig. 2(a).

The investigation presented in this paper is concentrated on a compression-tension type of connection that is located very near the beam-to-column joint as shown in Fig. 2(b): FPC4. A similar connection, FPC3, has been developed, tested and published earlier (Hoenderkamp *et al*. 2012) and is used here for comparison purposes. For ease of construction and to improve the efficiency of the connections they are attached to the beams as close to the beam-column connections as possible. The connections are dry and will function immediately after assembly. They are located on the center line of the structural elements thereby keeping eccentricities to a minimum. Due to the gap between the concrete panel and the steel members, friction will not take place.

2. Interface connections FPC3 and FPC4

Compared to the previously used connections FPC1 and FPC2, an improvement could be obtained by placing frame-to-panel connections in the four corners of the steel frame at the column-beam junctions. The new connections would now have to be designed for tension and compression forces only. At these locations, as shown in Fig. 2(b), it is possible to develop a more efficient bracing system with complete X-bracing. To this purpose a push-pull connection type was developed and is shown in Fig. 3. This connection can be placed very close to the beam-to-column joints of the steel frame. The earlier designed and tested FPC3 consisted of five 16 mm diameter anchor bars (Feb500) welded to a 15 mm thick rectangular steel flange plate

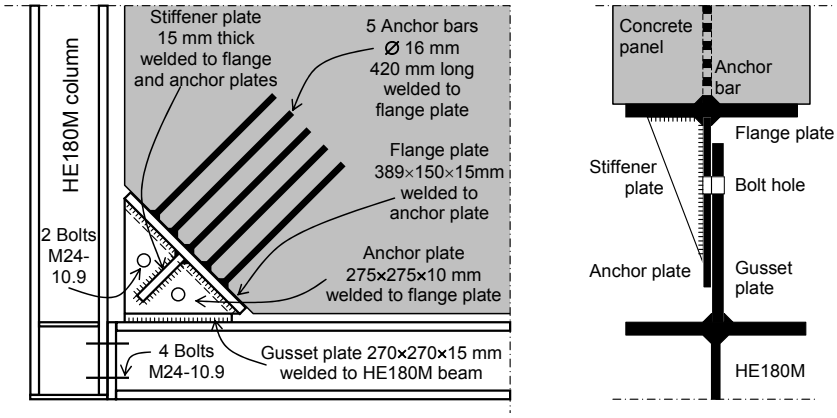

Fig. 3 Frame-panel-connection FPC4 (FPC3 is without the stiffener plate)

measuring 389 by 150 mm, perpendicular to the plane of the concrete panel. This plate is welded to a triangular anchor plate which is bolted to a triangular gusset plate using two 10.9 M24 bolts. The gusset plate is welded to the beam. In order to prevent buckling of the 10 mm thick anchor plate, a new frame-panel connection, FPC4, was designed with an additional 15 mm thick stiffener welded to the anchor and flange plates of the connection as shown in Fig. 3.

Individual tension tests on the frame-to-panel connections were performed to establish their load-displacement characteristics in tension. A schematic test set-up is shown in Fig. 4 which displays the dimensions of the concrete block. The set-up comprises a single concrete block that is placed on two jacks. The anchor plate is bolted to a steel holding strip replacing the gusset plate, which is connected to a test rig. Vertical displacements were measured on the anchor plate, the bolts and the concrete panel. Four connections were tested. Specific data for the materials are given in Table 1 where f_u is the ultimate strength and f_y is the yield stress. The compressive strength of the concrete, f_{ck}, was obtained from standard cube tests of 150×150×150 mm. The equivalent characteristic cylinder strengths are also given. Anchor plate movement and bolt hole ovalisation in the anchor plates are determining the connection behaviour. The modes of failure for all tension tests were identical: anchor pull-out.

Load-displacement measurements were done for several characteristic types of behaviour in the connection. This allows the connections to be accurately modeled for a finite element analysis of the complete infilled frame structure. It should be noted that the actual connections used in the full scale tests cannot be tested to failure beforehand. In addition to that, it can be expected that the

Table 1 Material properties of frame-to-panel connections

FPC	Bolts	Anchor bars FeB500		Anchor plates		Concrete panels	
	M24	∅ mm	f_u N/mm^2	f_y N/mm^2	f_u N/mm^2	Rebars ∅, mm	f_{ck} N/mm^2
FPC3 FPC4	10.9	16	500*	266	516	8 @ 150	58 45**

* nominal value, ** approximate cylinder strength

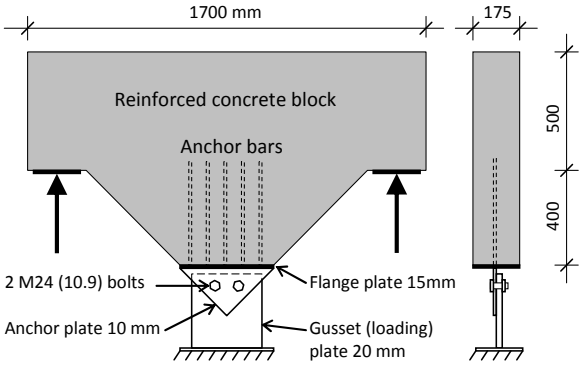

Fig. 4 Test set-up for connections; anchor pull-out and ovalisation

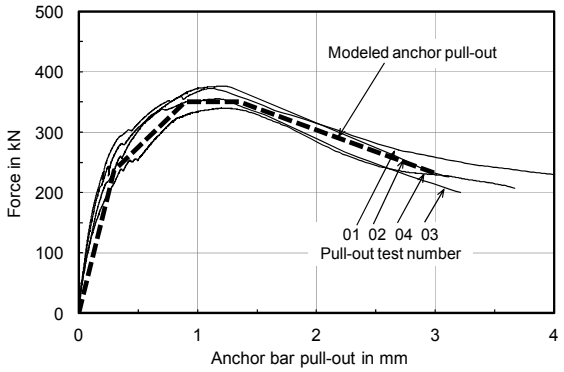

Fig. 5 Force vs. displacement due to anchor bar pull-out

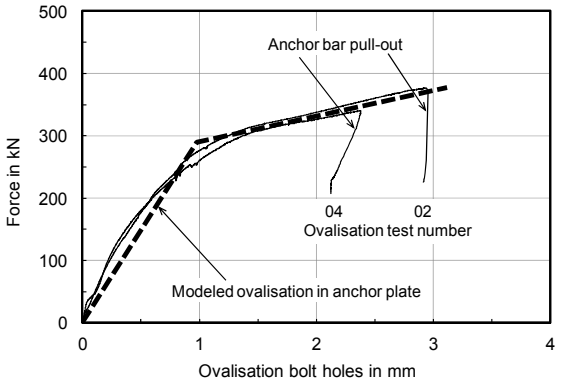

Fig. 6 Force vs. displacement due to ovalisation of bolt holes

properties of the materials used in the connection tests are dissimilar to those of the materials of the full scale tests. Fig. 5 shows four load displacement curves for anchor bar slip in the concrete block. The typical characteristics of the anchor bar behaviour in the concrete are displayed by the modeled pull-out curve in the diagram.

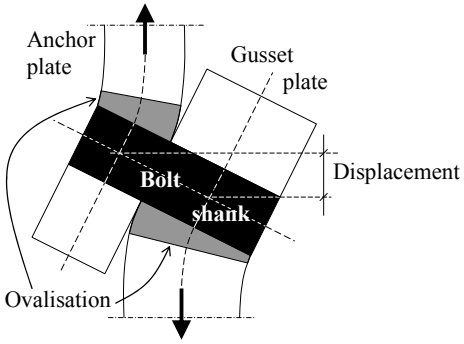

Fig. 7 Displacement due to rotation of bolt shank

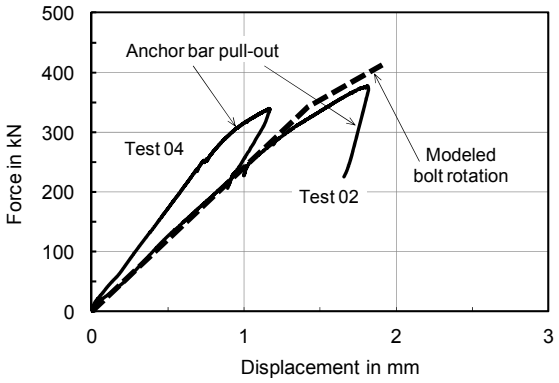

Fig. 8 Force vs. displacement due to bolt shank rotation

The ovalisation of the bolt holes needed to be measured on both sides of the plates because of rotation of the bolts. This rotation is caused by bending in both the anchor and gusset plates as is shown in Fig. 7. It occurs in the connections subject to tension as well as in the connections in compression. Successful measurements were only obtained for two tests as shown in Fig. 6. Again, the typical characteristics of bolt hole ovalisation in the anchor plates are displayed by a modeled ovalisation curve.

The displacements due to rotation of the bolt shanks in the connection have also been measured during the tests. It is clearly shown in Fig. 7 that the rotation results from bending in the gusset and anchor plates. Like the ovalisation measurements it resulted in only two sets of useful data as shown in Fig. 8. The curve “Modeled bolt rotation” is taken to represent its typical characteristics.

The modeled curves represent three characteristic modes of behaviour in the connection. They allow the strength and stiffness of similar connections in full-scale infilled frame tests, but with different material properties, to be determined for analysis of this frame.

3. Full scale infilled frame test with FPC4

A full scale infilled frame test with FPC4 connections was carried out in a specially designed test rig for infilled frames as shown in Fig. 9. The rig consists of a vertical and a diagonal loop

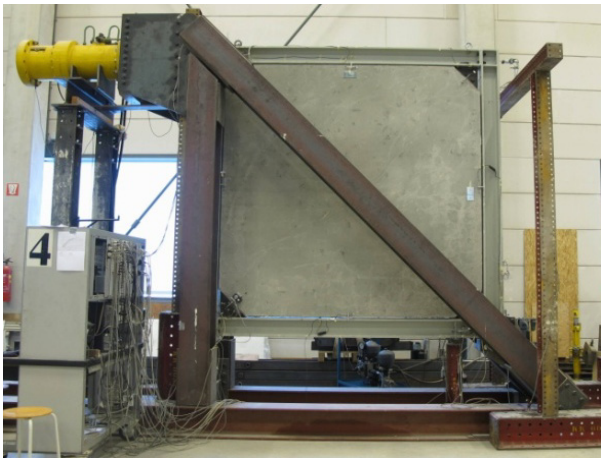

Fig. 9 Full scale test set-up

assembled from HE300B sections. At the top left corner of the test rig a hydraulic jack is mounted, with a capacity of 2 MN and a maximum stroke of 200 mm. At the lower left corner of the test rig the test specimen will be supported in vertical direction only to simulate a roller support. Four steel M30 threaded rods are used to transfer vertical loads to the vertical loop of the test rig and they permit rotation and horizontal translation of the test specimen. At the lower right corner of the test rig, the specimen is supported in a steel block or saddle. This support acts like a hinged connection and only allows the test specimen to rotate in its plane at this location, thus lateral and vertical translations are restricted here. The test specimen is loaded in one direction only.

The steel frame of the infilled structure to be tested consists of four HE180M steel sections (S235), two beams and two columns. The beams are connected to the columns with four M24 10.9 bolts as shown in Fig. 3. The bolts are tightened up to a maximum torque of 400 Nm, to obtain an identical rotational stiffness at each beam to column connection. Triangular gusset plates are welded to the beams near the frame corners for connection to the concrete panel. For the 2760 mm square infill panel C35/45 concrete was used to cast a slab with a thickness of 200 mm including a cover of 25 mm. The panel is reinforced with a ∅8-150 FeB500 mesh on both sides. Along the panel edges reinforcement hooks ∅8-150 FeB500 were placed. The compressive strength of the concrete was determined on the day the full scale experiment was carried out. Table 2 gives the properties of the steel and concrete used in the testing of individual connections FPC3 and FPC4 in addition to the material properties used for the connections and the infill panel in the full scale frame test.

The bare steel frame was tested first to determine its contribution to the stiffness of the infilled frame. It was loaded up to 80 kN to deform the frame elastically only thereby avoiding any damage which could affect the behaviour of the infilled frame during the full scale test. The load displacement curve in Fig. 10 displays a non-linear stage up until about 40 kN. Thereafter a linear branch can be observed which represents the lateral stiffness of the bare frame: 2.3 kN/mm. This is the contribution of the bare frame to the overall horizontal stiffness of the infilled frame.

The second and third tests (C and D) were performed on full scale infilled frames with FPC3 and FPC4 respectively. After testing the bare frame, the concrete infill panel is connected to the steel frame in a horizontal position at floor level. At the beginning of the infilled frame tests, the

Table 2 Changes in material properties of frame-to-panel connections

Test	Anchor plate		Gusset plate			Concrete panel		
	f_y N/mm^2	f_u N/mm^2	f_y N/mm^2	f_u N/mm^2	thickness mm	f_{ck} N/mm^2	E_c kN/mm^2	thickness mm
Material properties of individually tested connections								
FPC3 FPC4	266	516	-	-	20	58	28.9	175
Properties of connection materials in full scale infilled frame tests								
Test C with FPC3	314	515	470	538	15	64	32.1	200
Test D with FPC4	314	515	470	538	15	74	31.4	200

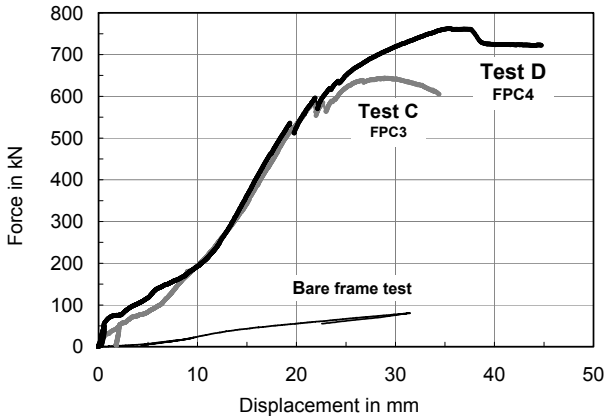

Fig. 10 Load vs. maximum horizontal displacements for full scale tests

specimens are subjected to a preload of 50 kN to take out the possible slack between bolts and bolt holes of the interface connections. After unloading, the infilled frames are loaded again up to failure under controlled displacement at 1 mm/min. The load-displacement curves in Fig. 10 show the lateral structural behaviour of the two tests. The load-displacement curves in Fig. 10 show the lateral structural behaviour of Test C with frame panel connection FPC3, Test D with FPC4 and a test on the bare frame.

The settling-in stage of the two infilled frame structures until ±200 kN is a combination of closing the initial gap between test specimen and test rig, and a non-simultaneous on-set of contact between bolt shanks and steel for the eight bolts connecting the four gusset plates to the four anchor plates.

The behaviour of specimen C is almost linear up to 584 kN with an initial stiffness of 34.8 kN/mm. Then the first crack in the tension diagonal of the concrete panel occurs near the ends of the 420 mm long anchor bars of the upper ‘tension connection’. After a small drop the lateral load again increases to 585 kN when a crack at the opposite corner in the tension diagonal occurs which is also located at the end of the anchor bars and this causes an additional small load drop. The

Table 3 Structural properties of infilled steel frames

	Yielding level, kN	Ultimate strength, kN	Lateral stiffness, kN/mm
Test C	584	644	34.8
Test D	536	762	40.7

lateral load increases to a maximum of 644 kN at a deflection of 28.9 mm. After reaching this strength, large out of plane deformations were observed in the anchor and the gusset plates of the frame panel connection in the lower compression corner. This resulted in a decreasing load and increasing lateral displacements as clearly indicated by the curve in Fig. 10.

The behaviour of specimen D can be considered linear up to 536 kN with an initial stiffness of 40.7 kN/mm. At this load the first crack in the tension diagonal of the concrete panel occurs near the ends of the 420 mm long anchor bars of the upper 'tension connection'. After a load drop of 23 kN the lateral load again increases to 596 kN when a crack at the opposite corner in the tension diagonal occurs. This crack is also located at the end of the anchor bars and caused a load drop of 24 kN. From this point on, the lateral load increases to 762 kN with a deflection of 35.3 mm. This is followed by anchor bar pull-out and soon after by panel-frame contact. For practical reasons the test was halted at 722 kN giving a horizontal displacement of 44.7 mm.

Salient data obtained from the two infilled frame tests are given in Table 3. It is clearly shown that adding stiffener plates to the frame panel connections in Test D improves the strength and stiffness of the infilled frame.

4. Finite element analysis of infilled frames

A simple finite element model as shown in Fig. 11 was developed for simulating the racking shear behaviour of Test D with connections FPC4. The set up of the finite element model is presented in the following order: steel frame and precast concrete infill panel, frame-panel connection, and infilled frame. For these three parts, the applied elements, element geometry, and material characteristics are discussed.

4.1 Steel frame and precast concrete infill panel

Two-node beam elements, which have a fourth-order shape (deflection) function, are used to model the beams and columns of the steel frame. A node of these elements has three degrees of freedom: translation in the nodal x and y directions and rotation about the nodal z-axis. The bolted connections between the beams and columns of the steel frame are replaced by rotational springs in the finite element analysis as shown in Fig. 11.

The applied rotational spring is a simple and purely rotational element with three degrees of freedom at each node, however, in the finite element model only the rotations about the nodal z-axis are admitted. It provides a relationship between moment and rotation via a moment-rotation diagram. The relative translation in x and y directions will be restricted by constraints For the beams and columns nominal values of HE180M sections are used: sectional area A = 11325 mm^2, sectional height h = 200 mm and moment of inertia I_y = 74830000 mm^4. The beams and columns are divided into thirty beam elements each. The rotational spring representing the bolted connection between the columns and beams is located at the end of a rigid offset that is connected

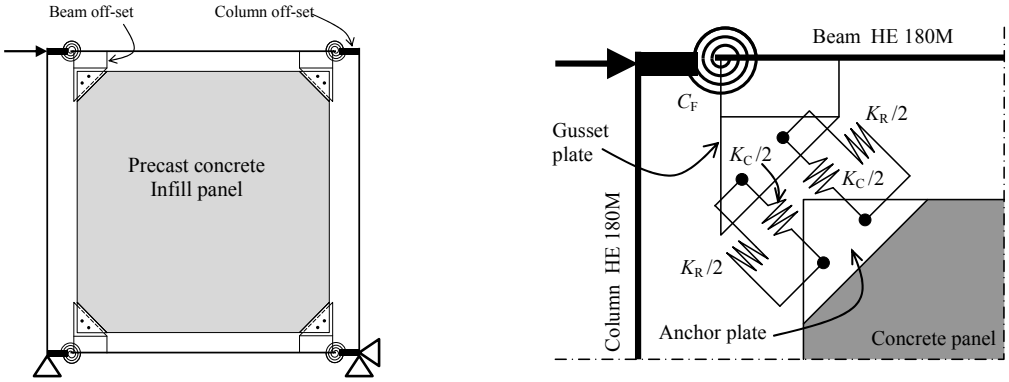

Fig. 11 Simplified finite element model of infilled frame

to the column end at the neutral axis of the beam. The material property that is used for the steel sections is Young's modulus E_s = 210000 N/mm^2 and Poisson's ratio = 0.3. The rotational spring characteristics (C_F) that represent the bolted connection between the beams and columns of the bare steel frame can be indirectly obtained from the force-deflection curve for the "Bare frame test" shown in Fig. 10. They are modeled with a bi-linear moment-rotation curve: the initial stiffness up to a bending moment of 28 kNm is 19640 kNm/rad, thereafter the stiffness is 8909 kNm/rad.

Plane stress elements are used to model the precast concrete panel. This higher order 2D plane stress element has 8 nodes for quadratic shaped elements and 6 nodes for triangular shaped elements. The element has two degrees of freedom at each node. These are translation in the nodal x and y directions. Quadratic elements are used where possible to model the geometry of the rectangular infill panel, however triangular elements are employed where the concrete panel connects to the anchor plate to accommodate the transition between the mesh of the concrete panel and the mesh of anchor plate. The material properties of the concrete have been experimentally determined, Young's modulus E_c is 31.4 kN/mm^2 and the Poisson's ratio is taken as 0.2.

4.2 Frame-to-panel connection

The offset, gusset and anchor plates of FPC4 shown in Fig. 11 are modeled with plane stress elements. They have a Young's modulus of 210000 N/mm^2 and their Poisson's ratio is 0.3. Triangular elements are used to model the gusset plate and anchor plate of the frame panel connection. The gusset plate is connected to an offset plate, which represents half the depth of the beam and is modeled with quadratic elements. The thickness of the gusset plate and offset plate is 15 mm. All other dimensions of the frame panel connection are shown in Fig. 3. The anchor plate is directly connected to the concrete panel to prevent deformations between the two components, i.e., movement of the anchor bars is incorporated in the behaviour of the springs. The flange plate could thus be omitted in the analysis. Also note that the anchor plate stiffener cannot be modeled explicitly in a two-dimensional finite element analysis and this model does also not allow out-of-plane movements of the anchor plate. Spring elements are used to model 2 translational springs that represent diagonal action in compression, $K_C/2$ or $K_T/2$ (not shown) for tension. The tension action of the springs is used to model three specific modes of behavior in the connection: anchor slip/pull-out, ovalisation of the bolt holes and rotation of the bolt shanks due to asymmetric

loading in the connection. The compression spring stiffness K_C represents only bolt hole ovalisation and bolt shank rotation. To prevent rigid body rotation of the concrete panel, orthogonal springs are used with a combined stiffness K_R. This is identical to the compression stiffness of a connection as it is only subject to bolt hole ovalisation and bolt shank rotation since slip of the anchor bars does not occur in this direction. The experiment based load displacement curves for anchor bar pull-out, bolt hole ovalisation and bolt shank rotation are shown in Figs. 5, 6 and 8. They were obtained for material properties given in Table 1.

As shown in Table 2, the properties of steel and concrete used in the full-scale infilled frame test were not the same as used in the connection tests. It is therefore necessary to adjust the experimentally based load displacement curves of the three specific modes of behaviour of the connection in order to obtain correct input data for the finite element model of the full scale infilled frame.

4.2.1 Anchor bar pull-out

The modeled anchor pull-out curve in Fig. 5 is shown again in Fig. 12 by the dashed line. The adaptation of the load displacement curve can be obtained by applying an earlier proposed equation (Wang 2009) that relates the anchor pull-out to the concrete compressive strength, the cover of the anchor bolts and their spacing, i.e.

$$\frac{\ell_{\mathrm{d}}}{d_{\mathrm{b}}} = \frac{1.85\, f_{\mathrm{y}}}{\left(\dfrac{c + b_{\mathrm{e}}/3}{d_{\mathrm{b}}}\right)\sqrt{f_c'}} \tag{1}$$

where ℓ_{d} and d_{b} are the length and the diameter of the anchor bar respectively, c is the concrete cover, b_e is the anchor bar spacing, f_y is the yield strength of the bar and f'_c is the concrete compressive strength. For all connection tests and the infilled frame test the spacing, diameter, and length of the anchor bars remained unchanged. It is suggested that the yield strength of the anchor bar, represented by f_y in Eq. (1), be replaced by the actual stress F/A, i.e., the tensile force F in the anchor bar divided by its sectional area A. With the known changes in concrete cover, Eq. (1) can be rewritten as follows

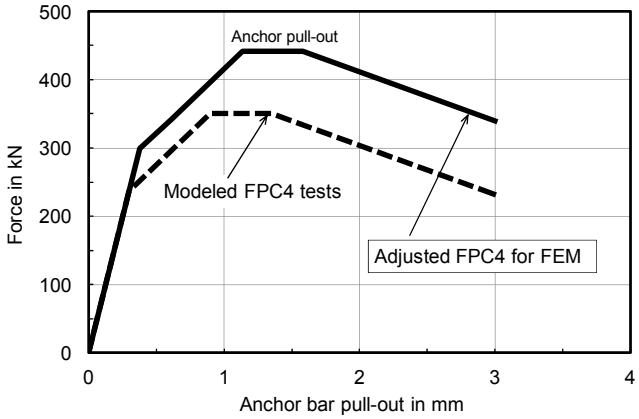

Fig. 12 Adjusting force-displacement curve for anchor bar pull-out

$$\left\{\frac{\frac{F}{A}}{\left(\frac{c+b_e/3}{d_b}\right)\sqrt{f_c'}}\right\}_{\text{FPC4}} = \left\{\frac{\frac{F}{A}}{\left(\frac{c+b_e/3}{d_b}\right)\sqrt{f_c'}}\right\}_{\text{Infilled Frame}} \tag{2}$$

Substituting and using the known pull-out load from the connection tests will yield an adjusted anchor bar capacity.

$$\left\{\frac{\frac{350}{1004}}{\left(\frac{80+65/3}{16}\right)\sqrt{58}}\right\}_{\text{FPC4}} = \left\{\frac{\frac{F}{1004}}{\left(\frac{92+65/3}{16}\right)\sqrt{74}}\right\}_{\text{Infilled Frame}} \tag{3}$$

The adjusted pull-out load of the anchor bars in a single connection for the full scale test is 441 kN. This is an increase of 26% compared to the maximum force of the bars in the connection tests at 350 kN. It is suggested that the forces of the anchor bar slip curve be increased with 26% leaving the four slopes of the curve unchanged, see Fig. 12. It is taken that the small change in the modulus of elasticity for concrete has little influence on the pull-out characteristics and is therefore ignored.

4.2.2 Bolt hole ovalisation

Fig. 13 displays a bi-linear relation "Ovalisation in anchor plate (a)" as a dashed line. This modeled curve is derived from the force-displacement curve for bolt hole ovalisation shown in Fig. 6. The steel used for the anchor plates in the full scale tests was of a higher grade compared to the material used in the connection tests, Table 2. This requires an alteration to the modeled experimental force-displacement curve.

The ratio between the yield stresses of the anchor plates used for the individual FPC4 testing and for the connections used in the infilled frame test is used to adjust the yielding level of the bolt hole ovalisation as follows

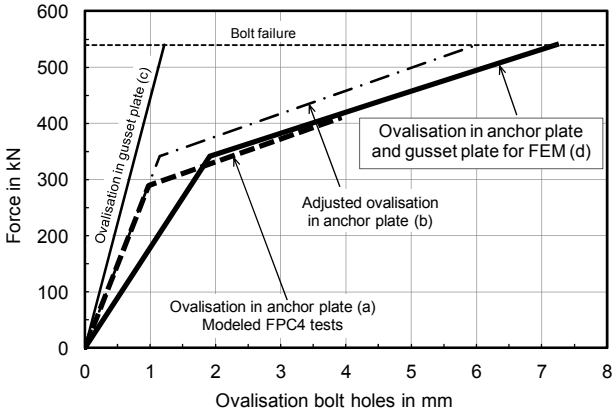

Fig. 13 Adjusting force-displacement curve for ovalisation of bolt holes

$$F_{AP} = \frac{f_y}{f_{y;FPC4}} F_{FPC4} = \frac{314}{266} \times 290 = 342 \text{ kN} \tag{4}$$

where F_{FPC4} is the yield level of ovalisation for the "Modeled FPC4 tests" shown in Fig. 13 and F_{AP} is the adjusted yield level of ovalisation in the anchor plate.

It is assumed that the initial elastic stiffness and subsequent plastic stiffness remain unchanged. This leads to the curve "Adjusted ovalisation in anchor plate (b)". Due to early anchor pull-out the ultimate ovalisation load at rupture could not be obtained. Instead, the ultimate load is now set at the theoretical shear resistance of the two M10.9 bolts in the connection (bolt failure)

$$F_{v;Rd} = 2\alpha_v f_{ub} A = 2 \times 0.6 \times 1000 \times 452 \times 10^{-3} = 540 \text{ kN} \tag{5}$$

in which α_v is a factor depending on the location of the shear plane (α_v = 0.6 for shear plane passing through the unthreaded portion of the bolt), f_{ub} is the ultimate strength of the bolt material and A is the gross cross section of the bolt if the shear plane passes through the unthreaded portion of the bolt. This load is beyond the actual loading of the connection in the full scale test and is not expected to be reached in the finite element analysis as well.

The deformation characteristics of ovalisation in the 20 mm thick loading (gusset) plate used in the FPC4 tests are unknown. It is therefore suggested that the force-ovalisation behaviour of the 15 mm thick gusset plates used in the frame analysis be derived from properties of the material of the 10 mm thick anchor plates used in the full scale tests by increasing its initial stiffness by 33%. It is taken that the yielding level of the gusset plate F_{GP} changes proportionally to the yielding level of anchor plate F_{AP} according to their yield stress ratio, i.e.

$$F_{GP} = \frac{f_{y;GP}}{f_{y;AP}} F_{AP} = \frac{470}{314} \times 342 = 512 \text{ kN} \tag{6}$$

The plastic behaviour of the ovalisation in the gusset plate is omitted here since the elastic strength of 512 kN is about 5% below the theoretical shear resistance of the bolts, at 540 kN. This allows the relationship "Ovalisation in gusset plate (c)" to be set up as shown in Fig. 13. The curve "Ovalisation in anchor plate and gusset plate for FEM (d)" can now quite easily be obtained by adding curves (b) and (c).

4.2.3 Bolt rotation

Due to asymmetric forces in the frame panel connection the gusset plate and anchor plate will bend. This leads to rotation of the bolt shanks and causes a displacement in the frame panel connection as shown in Fig. 7. The "Modeled bolt shank rotation" curve shown in Fig. 8 for a 10 mm thick anchor plate and a 20 mm thick loading (gusset) plate is presented again in Fig. 14 as dashed line "Modeled FPC4 tests". As the thickness of the gusset plate used in the full scale test is only 15 mm, the force displacement behaviour of the bolt rotation needs to be altered. The following procedure is suggested. The bending stiffness ratio of the plates used in the full scale test, 10 mm + 15 mm thick, and the plates of the connection test, 10 mm + 20 mm thick, can simply be expressed as a ratio of the sum of their second moments of area

$$\frac{K_{\text{Infilled Frame}}}{K_{\text{FPC4}}} = \frac{10^3 + 15^3}{10^3 + 20^3} = 0.486 \tag{7}$$

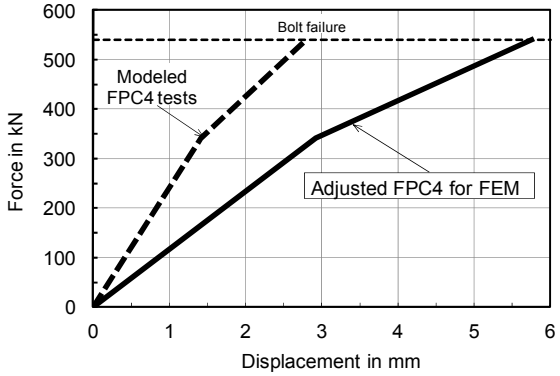

Fig. 14 Adjusted curve for bolt rotation and total force-displacement curves

It is suggested that the force-displacement curve for bolt rotation be adjusted accordingly. This leads to the FEM input curve shown in Fig. 14.

There are two additional phenomena that need to be addressed but are considered to have a minor influence on the bolt rotation characteristics and have been ignored in further analyses. The thinner gusset plate used in the full scale frame test creates a smaller moment arm between the neutral lines of the connection plates, see Fig. 7. This causes smaller bending moments and thus smaller bolt rotations. Additionally, the yielding levels in the two connection tests for bolt rotation were difficult to obtain as anchor pull-out occurred earlier than expected. For simplicity the yielding levels for bolt rotation have been set at the adjusted yield level value of ovalisation as shown in Fig. 13 and in Eq. (4) at 342 kN.

4.2.4 Adjusted force versus displacement curves

The separate force-displacement characteristics of anchor bar slip, bolt hole ovalisation, and bolt shank rotation are shown together in the diagram of Fig. 15. They are combined to form a spring stiffness for tension, K_T. The spring stiffness for compression, K_C consists of a combination of bolt hole ovalisation and bolt shank rotation since anchor bar slip does not occur under compression.

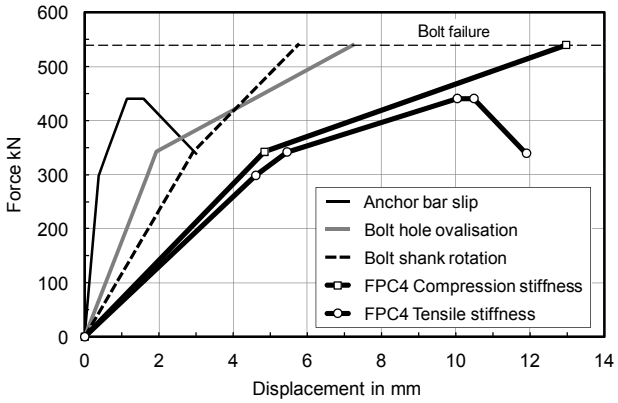

Fig. 15 Adjusted curves for total force-displacement curves

Table 4 Adjusted structural properties of FPC4

FPC	Tension		Compression	
	Stiffness K_p, kN/mm	Strength[(1)] $F_{p;u}$, kN	Stiffness K_s, kN/mm	Strength[(2)] $F_{s;u}$, kN
FPC4	64.8/51.5/21.6/0.0/-71.6[(3)]	441	70.1/24.4[(3)]	540

[(1)] anchor pull-out, [(2)] theoretical bolt failure, [(3)] multi-linear elastic-plastic

The two spring characteristics for tension and compression can be combined into one overall spring characteristic for use in the finite element model. The decreasing stiffness of the spring characteristic after anchor bar pull-out will be reduced to avoid convergence problems during the finite element analysis, i.e., the negative slope of the multi-linear curve is to be reduced. Table 4 shows the structural properties of FPC4.

4.3 Full infilled frame analysis

The lateral load of the experimental test is simulated by a prescribed horizontal displacement in the finite element analysis. Thus the loading is displacement controlled, since the load displacement tangent is expected to become negative, see Fig. 10. It should be noted that the settling-in phase observed in the full scale test is not included in the numerical analysis. Geometric non-linearity is taken into account. Material non-linearity for the steel and concrete used is not taken into account. However, the nonlinear springs, for which the behaviour is shown in Fig. 15, include the effects of e.g., ovalisation, which means that plasticity is described implicitly. Fig. 16 shows the load-deflection curve of the full-scale infilled frame obtained from the finite element analysis. It has been off-set to the right to accommodate a more direct comparison with the results of Test D. Plastic ovalisation of the bolt holes first occurred at the compression corners at 538 kN shortly followed by plastic ovalisation of the bolt holes at tension corners at 586 kN. This caused a substantial reduction of the lateral stiffness. The yielding level is taken to occur at the intersection of the elastic and plastic gradients, i.e., at 528 kN. This compares well to the yielding level of 536 kN for Test D, i.e., a 1% underestimate. The elastic stiffness obtained from the finite element

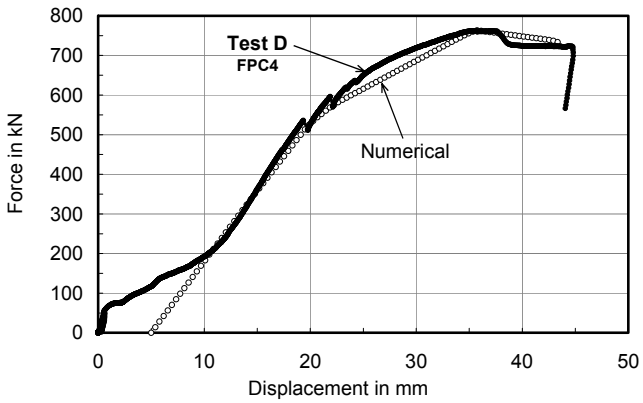

Fig. 16 Force vs. horizontal deflection of infilled frame

Table 5 Structural properties infilled frame

	Yielding level (kN)			Ultimate strength (kN)			Lateral stiffness (kN/mm)		
	Experiment	Numerical analysis	% difference	Experiment	Numerical analysis	% difference	Experiment	Numerical analysis	% difference
Test C with FPC3	584	555	-5	644	721	+12	34.8	34.0	-2
Test D with FPC4	536	528	-1	762	761	-0	40.7	35.8	-12
% difference	-8	-5	-	+18	+6	-	+17	+5	-

simulation at 35.8 kN/mm underestimates the experimentally obtained value of 40.7 kN/mm by 12%. In the simulation the first anchor bar pull-out occurs at the bottom tension connection at 761 kN. The numerically computed ultimate load is roughly the same as the test value. Additional results are given in Table 5 together with earlier published results for Test C (Hoenderkamp *et al*. 2012).

5. Conclusions

An improved frame-to-panel connection FPC4 for a corner connected precast concrete infill panel in a steel frame has been presented. This redesign has been tested in a full-scale infilled frame. Its performance in a one-bay-one-story full-scale frame subjected to in-plane horizontal loading has been compared to a numerical analysis and an identical infilled frame with earlier designed standard connections FPC3. The horizontal structural properties of this new composite structure show a significant improvement over the earlier infilled frame with an 18% increase in ultimate strength and a 17% increase in lateral stiffness.

The full-scale infilled frame has been modeled for finite element analysis. Mechanical properties of the discrete interface connection were obtained from experiments on individual connections. This allowed characteristic properties for stiffness and strength of the connection to be represented by multi-linear translational springs. It was shown that the numerically obtained structural properties of the infilled frame compare well with experimental results. Although only two full scale experiments have been simulated, it shows that this simple finite element model allows a systematic investigation of the influence of connections on the overall behaviour of steel frames with discretely connected precast concrete infill panels subject to in-plane lateral loading.

Furthermore, the full-scale experimental test shows that a precast concrete panel in a semi-integral infilled steel framed structure with discrete frame-panel connections in the four corners of the frame can significantly improve the lateral stiffness of bare steel frames. The lateral stiffness of the infilled frame structure after the settling-in phase, is 40.7/2.3 or roughly 18 times the bare frame stiffness.

The lateral stiffness and ultimate strength of the infilled structure were governed, as intended by design, by the discrete frame-panel connections.

References

Barua, H.K. and Mallick, S.K. (1977), "Behaviour of mortar infilled steel frames under lateral load", *Build. Environ.*, **12**(4), 263-272.

Benjamin, J.R. and Williams, H.A. (1958), "The behaviour of one-story reinforced concrete shear walls", *J. Struct. Eng., ASCE*, **84**(4), 1-29.

Dawe, J.L. and Seah, C.K. (1989), "Behaviour of masonry infilled steel frames", *J. Can. Soc. Civil Eng.*, **16**(6), 865-876.

Hoenderkamp, J.C.D., Hofmeyer, H. and Snijder, H.H. (2010), "Experimental investigation of the shear resistance of steel frames with precast concrete infill panels", *Adv. Steel Construct.*, **6**(3), 817-830.

Hoenderkamp, J.C.D., Snijder, H.H. and Hofmeyer, H. (2012), "Push-pull connections in steel frames with precast concrete infill panels", *The Open Construct. Build. Technol. J.*, **6**(1), 63-73.

Holmes, M. (1961), "Steel frames with brickwork and concrete infilling", *Proc. Insti. Civ. Engrs.*, **19**(4), 473-478.

Liauw, T.C. and Kwan, K.H. (1983), "Plastic theory of infilled frames with finite interface shear strength", *Proc. Insti. Civ. Engrs.*, Part 2, **75**(4), 707-723.

Liauw, T.C. and Kwan, K.H. (1984), "Nonlinear behaviour of non-integral infilled frames", *Comput. Struct.*, **18**(3), 551-560.

Liauw, T.C. and Lo, C.Q. (1988), "Multibay infilled frames without shear connectors", *J. Am. Concrete Inst.*, **85**(4), 423-428.

Mallick, D.V. and Garg, R.P. (1971), "Effect of openings on the lateral stiffness of infilled frames", *Proc. Insti. Civil Engrs.*, **49**(2), 193-210.

Ng'andu, B.M., Martens, D.R.W. and Vermeltfoort, A.T. (2006), "The contribution of casiel infill walls to the shear resistance of steel frames", *Heron*, **51**(4), 201-223.

Polyakov, S.V. (1960), "On the interaction between masonry filler walls and enclosing frame when loaded in the plane of the wall", English translation in *Earthquake Engineering*, Earthquake Engineering Research Institute, San Francisco, CA, USA, pp. 36-42.

Stafford Smith, B. (1962), "Lateral stiffness of infilled frames", *J. Struct. Div. ASCE*, **88**(6), 183-199.

Stafford Smith, B. (1966), "Behaviour of square infilled frames", *J. Struct. Div., ASCE*, **92**(1), 381-403.

Stafford Smith, B. (1967), "Methods for predicting the lateral stiffness and strength of multi-storey infilled frames", *Build. Sci.*, **2**(3), 247-257.

Teeuwen, P.A., Kleinman, C.S., Snijder, H.H. and Hofmeyer, H. (2008), "Full-scale testing of infilled steel frames with precast concrete panels provided with a window opening", *Heron*, **53**(4), 195-224.

Teeuwen, P.A., Kleinman, C.S., Snijder, H.H. and Hofmeyer, H. (2010), "Experimental and numerical investigations into the composite behaviour of steel frames and precast concrete infill panels with window openings", *Steel Compos. Struct., Int. J.*, **10**(1), 1-21.

Thomas, F.G. (1953), "The strength of brickwork", *Struct. Eng.*, **31**(2), 35-46.

Wang, H. (2009), "An analytical study of bond strength associated with splitting of concrete cover", *Eng. Struct.*, **31**(4), 968-975.

DL